SANDIA REPORT
SAND2024-06978
Printed June 2024

Sandia National Laboratories

Heat Transfer Through a Box Beam from an Impinging Hydrogen Flame

Gabriela Bran Anleu, Myra Blaylock, Benjamin Schroeder, Chris LaFleur

Prepared by
Sandia National Laboratories
Albuquerque, New Mexico
87185 and Livermore,
California 94550

Issued by Sandia National Laboratories, operated for the United States Department of Energy by National Technology & Engineering Solutions of Sandia, LLC.

Available to DOE and DOE contractors from
U.S. Department of Energy
Office of Scientific and Technical Information
P.O. Box 62
Oak Ridge, TN 37831

Telephone: (865) 576-8401
Facsimile: (865) 576-5728
E-Mail: reports@osti.gov
Online ordering: http://www.osti.gov/scitech

Available to the public from
U.S. Department of Commerce
National Technical Information Service
5301 Shawnee Rd
Alexandria, VA 22312

Telephone: (800) 553-6847
Facsimile: (703) 605-6900
E-Mail: orders@ntis.gov
Online order: https://classic.ntis.gov/help/order-methods/

ABSTRACT

An analysis was performed to determine whether a hydrogen jet flame impinging on a tunnel ceiling composed of multiple prestressed steel reinforced concrete box beams could result in permanent damage to the tunnel. The lower layer of the concrete box beam was modeled to determine whether heat reaches the steel reinforcing bars and whether spalling could occur. Heat transfer analysis shows that the temperature remains constant at the location of the steel reinforcing bars after 1.3 minutes of impingement and reaches a maximum of 130°C after 5 minutes. However, assuming a constant impingement for 5 minutes is an over estimation due the existing fire model which includes conservative assumptions. Explosive spalling may occur at a thin layer (~0.05 in. at 50 seconds, 0.1 in. at 5 minutes) at the bottom surface of the concrete box beam, but the steel reinforcing bars will not be exposed to the hydrogen flame.

ACKNOWLEDGEMENTS

This material is based upon work supported by the U.S. Department of Energy's Office of Energy Efficiency and Renewable Energy (EERE) under the Hydrogen and Fuel Cell Technologies Office (HFTO) Safety Codes and Standards sub-program, under the direction of Laura Hill. The authors also wish to thank Justin Slack and John Czach from the Massachusetts Department of Transportation (MassDOT) and Charles Myers from the Massachusetts Hydrogen Coalition for their help in providing tunnel information and feedback on the analysis. The authors gratefully acknowledge Melissa Louie, Marina Miletic, and Brian Ehrhart from Sandia National Laboratories for their review of this work.

CONTENTS

Abstract 3
Acknowledgements 4
Acronyms and Terms 8
1. Introduction 9
    1.1. Fire Scenario 10
    1.2. Previous CFD Simulations of Hydrogen Flame Impingement 10
    1.3. Tunnel Structure 11
        1.3.1. Material Properties 12
2. Numerical Simulations 15
    2.1. Numerical Domain 15
    2.2. Mathematical Model 16
        2.2.1. Energy Conservation Equation 16
        2.2.2. Initial and Boundary Conditions 16
    2.3. Mesh Refinement 17
3. Results 19
4. Summary and Conclusions 23
References 26
Distribution 27

LIST OF FIGURES

Figure 1: (a) Blowdown of a 125 L (0.125 m^3) high pressure hydrogen tank showing mass flow rate on the left blue axis and the hydrogen visible flame length [3] on the right red axis, and (b) the velocity of the blowdown for the tank with a 2.25 mm TPRD orifice [3]. (c) The total hydrogen mass released as a function of time for a 5.25 cm TPRD orifice and constant mass flow rate, showing when 5 kg are released. 11
Figure 2. Rear view of the ceiling structure shows prestressed concrete butted box beams alignment. Front view of the box beam (traffic goes into the page). Section at the end of the beam shows the dimension of the concrete box beam (steel reinforcing bars not shown) and the section that will be modeled (green box) [7]. 12
Figure 3. The ceiling structure is composed of adjacent prestressed concrete steel reinforced box beams of AASHTO Type BI-36, BI-48, or BII-48. Section at the end of the beam shows the dimension of the concrete box beam and the location of the steel reinforcing bars marked with a plus sign and bold lines [8]. 12
Figure 4. Temperature dependent a) density, b) specific heat, and c) thermal conductivity of dry concrete used in the heat transfer model of the box beams [6]. 13
Figure 5: Isometric view of concrete slab used in heat transfer model. The concrete slab has a length of 600 in. (1524 cm), a width of 280 in. (713 cm), and a thickness of 5.5 in. (14 cm). All surfaces are assumed to be insulated except the bottom surface where convection and radiation are prescribed. Temperature T1-T21 are located every 0.25 in. (0.64 cm) across the thickness of the concrete. (Figure not to scale) 15
Figure 6. Boundary conditions applied on bottom surface of tunnel ceiling structure: (a) temperature map from [1], (b) the radial temperature, (c) convective heat transfer coefficient,

and (d) irradiation plotted with respect to the r-axis measuring radial length from the center of the flame impingement at the bottom surface. 17
Figure 7. Temperature at y=0 (top-left), y=1 in. (top-right), 1.75 in. (bottom-left), and 5.5 in. (bottom-right) from the bottom surface for intervals 12 to 30. When the thickness is divided into 26 intervals or more, the mesh is sufficiently fine. 18
Figure 8. Isometric view of mesh for the lower concrete layer of the box beam using 26 intervals along the thickness of the concrete layer. 18
Figure 9. Temperature distribution across a 5.5 in. thick concrete slab at different time steps. From top to bottom: 0, 50 s, 1.3 min, and 5 min. Maximum and minimum values are specified for each time step. 19
Figure 10. Transient temperature profiles for different y-locations at $\boldsymbol{x} = \boldsymbol{z} = 0$ for the concrete slab in box beam tunnel. The red-dashed line indicates the maximum temperatue of the concrete. Figure 10b is a version of Figure 10a with a smaller y-axis temperature scale to show the increasing temperatures at locations y= 1.0 in. in purple and y = 1 ¾ in. in magenta from the bottom surface to emphasize the location where the steel reinforcing bars are located. 20
Figure 11. Temperature profiles across the thickness of the concrete slab in box beam at different time steps show that at y = 2 in. the temperature is still ambient. Locations y = 1.0 in. (purple) and y = 1 ¾ in. (magenta) are marked to show the location of the steel reinforcements. 21

LIST OF TABLES

Table 1. Summary of temperatures of the box beam tunnel at t = 50 seconds, 1.3 minutes, and 5 minutes. 25

This page left blank

ACRONYMS AND TERMS

Acronym/Term	Definition
AHJ	authority having jurisdiction
CFD	computational fluid dynamics
FCEV	fuel cell electric vehicle
NFPA	National Fire Protection Association
PDE	partial differential equation
TPRD	thermally-activated pressure relief device

1. INTRODUCTION

Hydrogen fuel cell electrical vehicles (FCEVs) can help reduce greenhouse emissions coming from the transportation sector as an alternative to gasoline vehicles [1]. The safety implications of this novel fuel should be considered for use cases where this fuel type would have different responses than typical gasoline or diesel fuels, such as in the case of the vehicle being in a fire in a tunnel. Chapter 7 of the National Fire Protection Association Standard for Road Tunnels, Bridges, and Other Limited Access Highways (NFPA 502) provides recommendations to ensure tunnel safety to the authority having jurisdiction (AHJ) [2], which is responsible for enforcing the requirements of a code or standard. NFPA 502 provides three main guidelines for concrete: a) concrete is protected from fire-induced spalling, b) temperature of the concrete surface does not exceed 380°C, and c) the temperature of the steel reinforcements within the concrete should not exceed 250°C. However, Annex G of NFPA 502 explains that these requirements do not consider alternative fuels, such as hydrogen. Instead, the requirements were developed for gasoline, ethanol, and diesel fuels. The differences between a hydrogen fire and gasoline fire are listed in the *U.S. National Clean Hydrogen Strategy and Roadmap* [1], but the most important differences are that (1) hydrogen releases from a light duty hydrogen FCEV last no more than 5 minutes and (2) the temperature of a hydrogen fire is significantly higher than the temperature of a gasoline fire. NFPA 502 entrusted the responsibility to the AHJ for deciding to allow alternative fueled vehicles to utilize their tunnels and establishing mitigation once they are approved. As stated in Chapter 4 and 7 of NFPA 502, the AHJ should perform an engineering analysis when the consequences of a fire are unclear. This engineering analysis should also be used to establish mitigations for those consequences. This report is the engineering analysis for tunnels with ceiling structure consisting of concrete box beams.

The AHJ for a tunnel structure consisting of multiple pre-stressed steel reinforced concrete box beams butted horizontally against each other was interested in learning about the severity of a specific low-probability, high-consequence scenario involving a hydrogen FCEV. This scenario consisted of a gasoline vehicle colliding with a hydrogen FCEV resulting in a hydrogen jet flame impinging on the tunnel ceiling structure [3]. In this work, we used numerical tools to investigate this scenario. The heat transfer within the concrete box beams was modeled using the thermal module, Aria, from the Sandia-developed Sierra suite [4]. The boundary conditions used in this study were obtained from a computational fluid dynamics (CFD) analysis performed by LaFleur et al. [3], where they modeled a hydrogen jet flame impinging on a flat ceiling surface with and without ventilation. Only the case without ventilation was considered here because it is the worst-case scenario. A mesh refinement study was performed to ensure that the temperatures obtained across the structure are independent of the mesh size.

The findings of this work can be used to determine whether the integrity of a tunnel with box beams will be compromised for the fire scenario described in Section 1.1. For similar tunnel structures, similar thermal behavior can be expected during a hydrogen jet flame impingement. Chapter 4 of the Code Requirements for Determining Fire Resistance of Concrete and Masonry Construction Assemblies Standard (ACI/TMS 216.1-14) [5] provides temperature dependent strength curves for different types of concrete and reinforcement steel bars. If the type of concrete and reinforcement steel bars are known, these curves can be used to determine whether their strength are compromised. To ensure that the findings of this report can be used to assess a specific tunnel, the assumptions and tunnel conditions used in this work should be carefully reviewed.

1.1. Fire Scenario

The low-probability high-consequence scenario of interest consists of a gasoline vehicle colliding with a hydrogen FCEV and overturning it. A fire caused by a gasoline leak triggers a release from the 125 L (0.125 m^3) high-pressure hydrogen tank's thermally-activated pressure relief device (TPRD). The TPRD releases the 5 kg of hydrogen from an orifice with a diameter of 2.25 mm in approximately 5 minutes as shown in Figure 1a (blue line). The combination of high pressure in the tank and the small TPRD orifice results in a choked flow with an average velocity of 700 m/s (see Figure 1b). Hydrogen ignites due to the heat from the gasoline fire resulting in a hydrogen jet flame [3]. The hydrogen jet flame impinges on the ceiling of the tunnel for about 1.3 minutes as shown in Figure 1a (red line). This scenario is conservative in that current light duty vehicles on the market have multiple, smaller tanks to hold the total 5 kg of hydrogen capacity so the tank blowdown of an actual vehicle would be a shorter duration and a smaller mass of hydrogen.

1.2. Previous CFD Simulations of Hydrogen Flame Impingement

The authors in [3] performed a CFD simulation of a hydrogen flame impinging on a flat surface located 16 ft from the tunnel ground. The heat flux from their CFD simulations serve as boundary conditions in the heat transfer simulations they performed on selected ceiling structures. To reduce the computational expense of the CFD simulations and reduce the Mach number at the orifice, the authors assumed a 5.25 cm TPRD orifice diameter (instead of 2.25 mm) and a constant velocity of 700 m/s (instead of the varying velocity shown in Figure 1b). Due to the high computational cost, the CFD simulations were run up to 3.3 seconds of release. At 3.3 seconds, the hydrogen jet flame had reached the ceiling of the tunnel, and the flame had reached stable conditions. The authors in [3] used the heat flux at 3.3 seconds as the constant boundary condition at the ceiling structure surface in their heat transfer simulations. The heat transfer simulations were run for 5 minutes, which represent the time a full 5 kg hydrogen tank takes to completely empty. Using a constant heat flux for duration of the release means that the mass flow rate at 3.3 seconds was also constant for the duration of the release. In other words, the blowdown shown in Figure 1a was not included in their heat transfer simulations. With this assumption, a total of 30 kg of hydrogen was released in 5 minutes instead of 5 kg. With a constant mass flow rate, 5 kg of hydrogen are released in only 50 seconds as shown in Figure 1c. This total mass parameter is also recognized as a further conservatism in the model.

In this work, the CFD results at 3.3 seconds are used as boundary conditions at the bottom surface of the ceiling structure. Temperatures at 50 seconds and 1.3 minutes are presented in this report, but results for a duration of 5 minutes are also noted. The heat transfer simulations do not model any spalling that may occur on the concrete due to the increase in temperature. Instead, previous concrete spalling experiments [6] were used to determine whether explosive spalling is likely to happen during the flame exposure. The authors in [6] found that explosive spalling can occur when concrete reaches temperatures higher than 750°C.

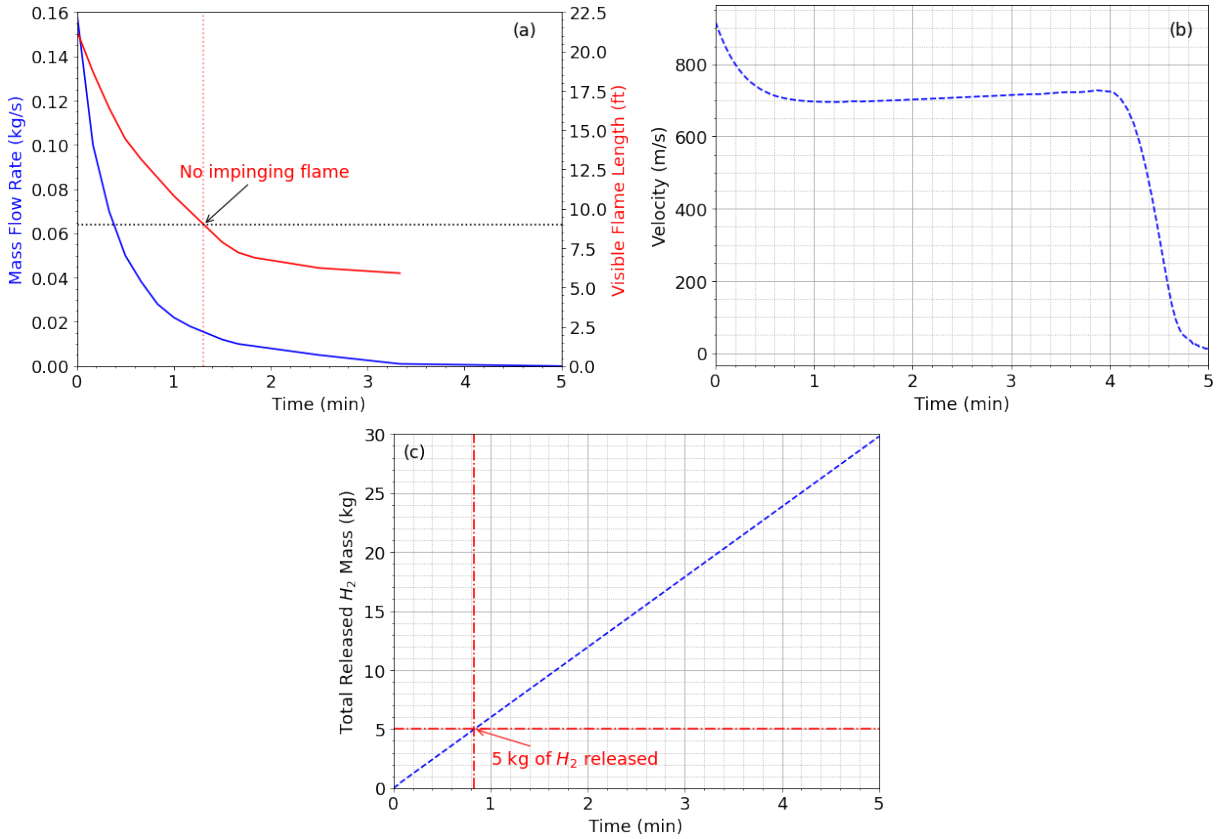

Figure 1: (a) Blowdown of a 125 L (0.125 m^3) high pressure hydrogen tank showing mass flow rate on the left blue axis and the hydrogen visible flame length [3] on the right red axis, and (b) the velocity of the blowdown for the tank with a 2.25 mm TPRD orifice [3]. (c) The total hydrogen mass released as a function of time for a 5.25 cm TPRD orifice and constant mass flow rate, showing when 5 kg are released.

1.3. Tunnel Structure

The tunnel in this analysis consists of two rectangular cells for traffic lanes as shown in Figure 3 [7]. Multiple prestressed steel reinforced concrete box beams butted horizontally against each other shape the ceiling structure (see Figure 2). AASHTO standard box beams of type BI-48, BII-48, or BI-36 [8] are commonly used in this type of tunnel structures. The dimensions of the box beams and the location of the steel reinforcing bars are specified on Figure 3 [7]. The steel reinforcing bars are located 1 in. (2.5 cm) and 1 ¾ in. (4.4 cm) from the bottom surface of the box beams.

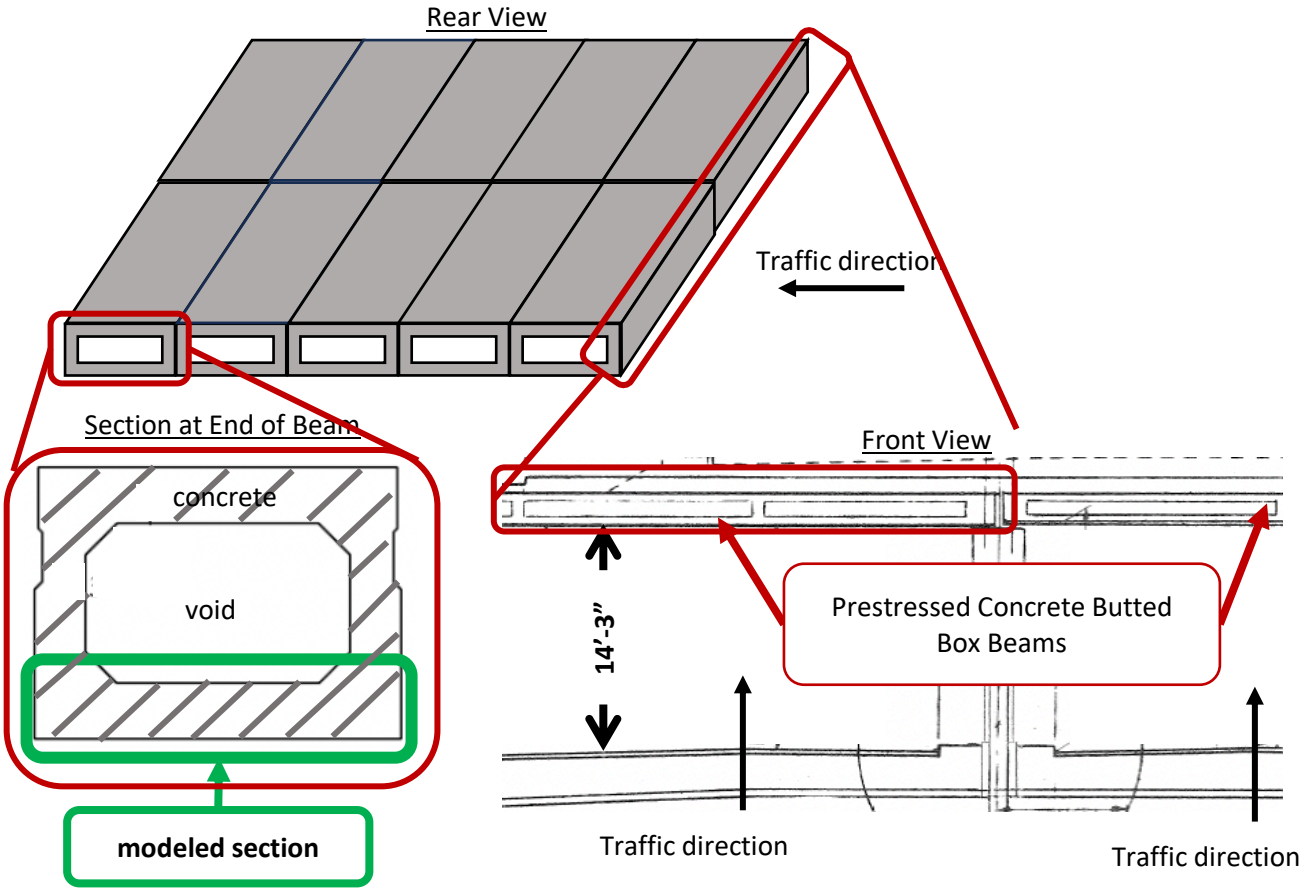

Figure 2. Rear view of the ceiling structure shows prestressed concrete butted box beams alignment. Front view of the box beam (traffic goes into the page). Section at the end of the beam shows the dimension of the concrete box beam (steel reinforcing bars not shown) and the section that will be modeled (green box) [7].

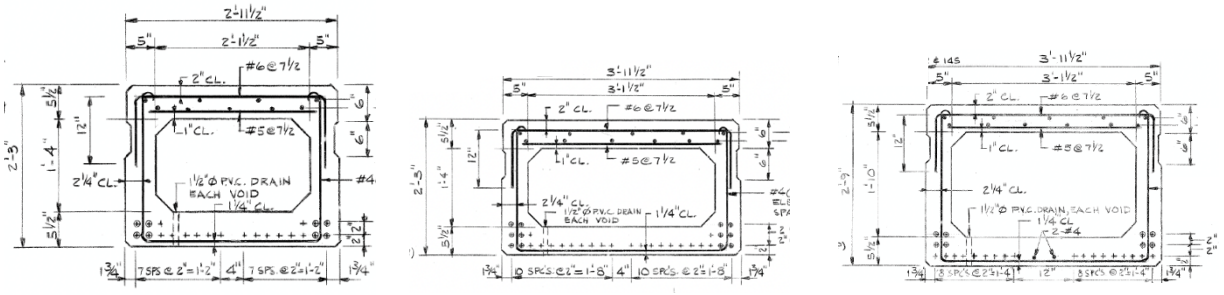

Figure 3. The ceiling structure is composed of adjacent prestressed concrete steel reinforced box beams of AASHTO Type BI-36, BI-48, or BII-48. Section at the end of the beam shows the dimension of the concrete box beam and the location of the steel reinforcing bars marked with a plus sign and bold lines [8].

1.3.1. Material Properties

The density, specific heat, and thermal conductivity of dry concrete used in the heat transfer model are shown in Figure 4a, b, and c, respectively. Values for density and thermal conductivity were not

available for temperatures higher than 1200°C, so the values at 1200°C were assumed for those higher temperatures. Specific heat values were not available for temperatures higher than 400°C, the specific heat values at 400°C were assumed for those higher temperatures.

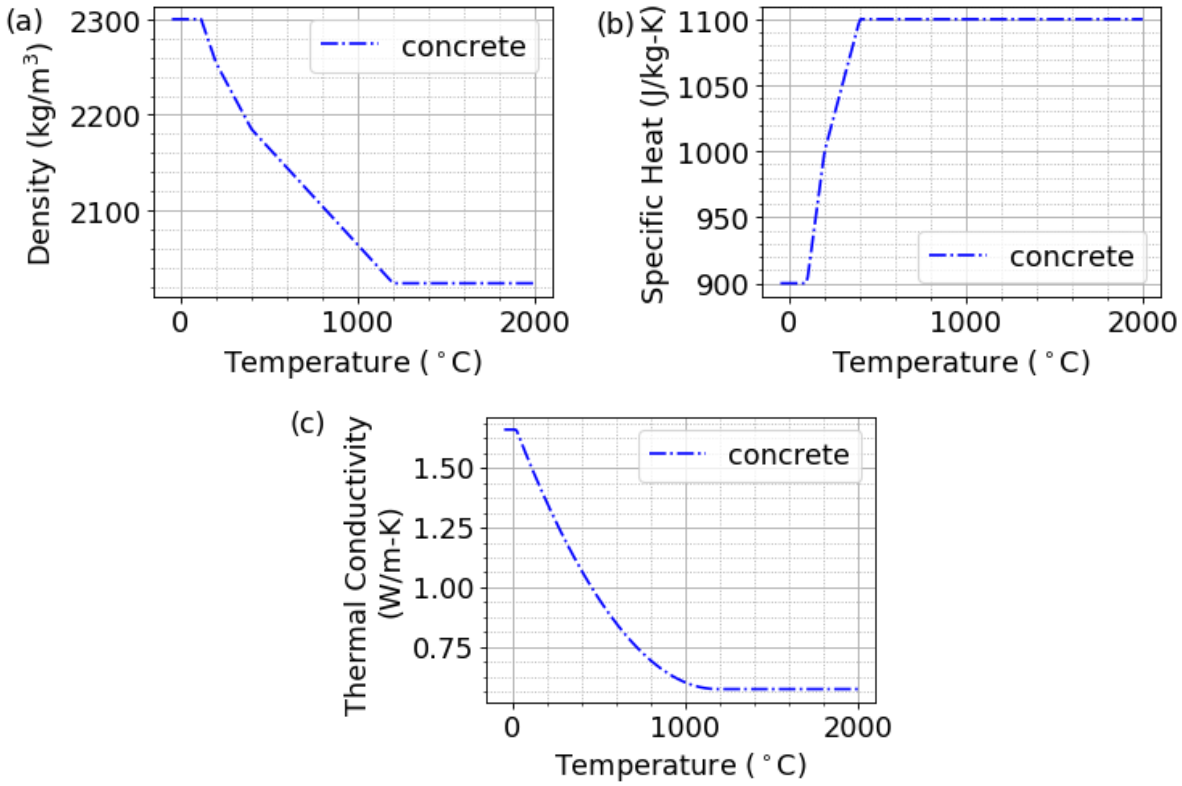

Figure 4. Temperature dependent a) density, b) specific heat, and c) thermal conductivity of dry concrete used in the heat transfer model of the box beams [6].

2. NUMERICAL SIMULATIONS

A heat transfer analysis was performed to determine whether the heat from the hydrogen jet flame could cause explosive spalling and could reach the steel reinforcing bars in the concrete box beam. Previous studies [3] found that concrete is an excellent insulator, so modeling just the concrete might be sufficient to determine whether the steel reinforcing bars would be compromised. Therefore, only the bottom section of the concrete box beam was modeled (green box shown in Figure 2). The steel reinforcing bars were not included in the heat transfer analysis. Instead, the temperature at the location of the steel reinforcing bars was highlighted to determine whether the steel reinforcing bars could lose their strength due to an increase in temperature. This simplification was used to determine whether further analysis was needed.

2.1. Numerical Domain

The numerical domain for the simulation was a rectangular slab with a length of 600 in. (1524 cm) and a width of 280 in. (713 cm), as shown in Figure 5. The thickness of the slab was th=5.5 in. (14 cm). The temporal temperature curves along the thickness of the slab for n=21 locations are presented in Section 3. Starting at the center of the bottom surface ($x = z = y = 0$), the temperature at every $\Delta y = 0.25$ in. (0.635 cm) was evaluated (see Figure 5). T_{21} is at $x = z = 0$ and $y = th$=5.5 in. (14 cm). T_5 and T_8 are the temperatures at 1 in. (2.54 cm) and 1 ¾ in. (4.45 cm), which are the locations of the steel reinforcing bars. Only the temperatures at x=z = 0 along y were plotted to show how the temperature increases along the thickness of the slab. These temperatures are not necessarily the maximum temperature along y as Figure 6 shows. However, the temperatures at $x = z = 0$ are relatively close to where the maximum temperature is predicted to occur, so the plotted temperatures give the reader a good estimate of how high the temperatures are at any given time. The maximum temperature of the whole structure as a function of time is also specified in Section 3.

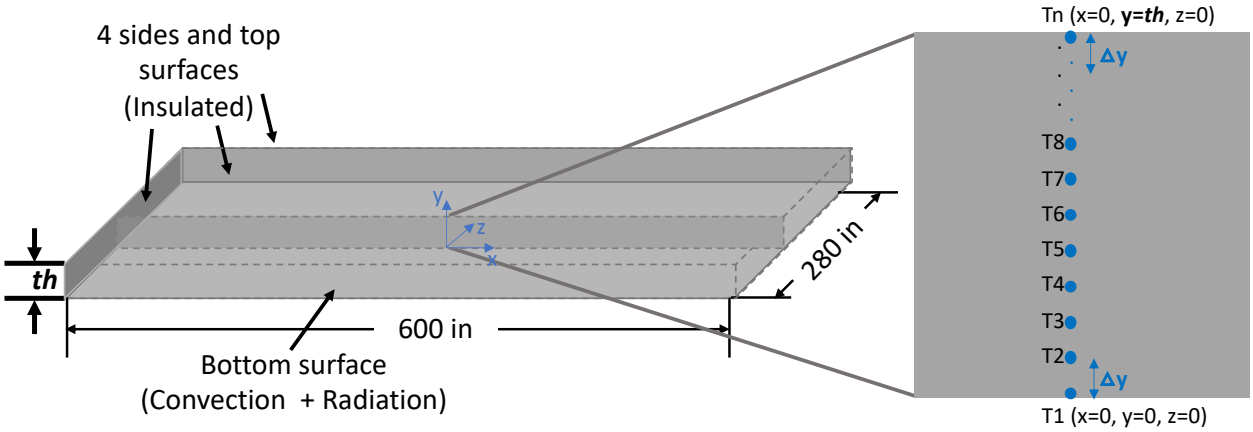

Figure 5: Isometric view of concrete slab used in heat transfer model. The concrete slab has a length of 600 in. (1524 cm), a width of 280 in. (713 cm), and a thickness of 5.5 in. (14 cm). All surfaces are assumed to be insulated except the bottom surface where convection and radiation are prescribed. Temperature T1-T21 are located every 0.25 in. (0.64 cm) across the thickness of the concrete. (Figure not to scale)

2.2. Mathematical Model

The Sierra module, Aria [4], was used to perform the heat transfer simulations. The model utilizes finite element method to numerically solve the three-dimensional unsteady partial differential energy equation (PDE).

2.2.1. Energy Conservation Equation

To solve for the temperature, $T(x, y, z, t)$, as a function of time (t) and position (x, y, z) within the slab, the following PDE was derived from an energy balance where the heat conduction in the slab is equal to the sensible heat stored in the slab,

$$\boldsymbol{\rho c_p \frac{\partial T}{\partial t} - \nabla \cdot (k \nabla T) = 0} \qquad \text{Equation 1}$$

where ρ is the bulk density, c_p is the specific heat, and k is the thermal conductivity of concrete. The Galerkin numerical method was used to discretize in space, and the finite difference method was used to discretize in time.

2.2.2. Initial and Boundary Conditions

The ceiling of the tunnel was assumed to have an initial ambient temperature, $T_{amb} = 25℃$,

$$T(t = 0) = T_{amb}. \qquad \text{Equation 2}$$

As shown in Figure 5, the structure was assumed to be insulated on all surfaces except for the bottom surface which encounters the hydrogen flame. In reality, the top surface will not be insulated since natural or forced (due to ventilation) convection and radiation losses will occur. However, assuming that the top is insulated defines a worst-case scenario. Convective and radiative heat transfer boundary conditions were applied at the bottom surface where the hydrogen jet flame impinges. The convective heat flux, $\dot{q}'''_{conv}$, applied to the surface is,

$$\dot{q}'''_{conv} = h(T_s - T_r) \qquad \text{Equation 3}$$

where T_s is the slab surface temperature, h is the heat transfer coefficient, and T_r is the gas reference temperature. The radiative surface heat flux, $q_{n,r}$, is defined as the thermal energy emitted from the surface minus the incident energy,

$$q_{n,r} = \epsilon(\sigma T^4 - G) \qquad \text{Equation 4}$$

where ϵ is the emissivity of concrete, σ is the Stefan-Boltzmann constant, and G is the irradiation. Because the previous CFD results for the no ventilation case showed that the hydrogen flame reaches a quasistatic state ~3.13 seconds into the simulation, the values for T_r, h, and G at 3.13 seconds (see Figure 6a were used as the boundary conditions for the proceeding heat transfer analysis [3]. These values were assumed to remain constant in time for the 5 minutes needed for the hydrogen tank to empty in a real blowdown scenario. This is a conservative assumption; in reality, as the mass flow rate of the hydrogen exiting the TPRD decreases, the values for T_r, h, and G would also decrease. A more extensive explanation on the results shown in Figure 6a can be found in [3]. To facilitate the mapping of the CFD boundary conditions on this new tunnel structure, the values along the r-axis in Figure 6a were mapped to the slab surface. The center of the hydrogen flame ($r=0$ in Figure 6a) was positioned at the center of the slab ($x=y=z=0$ in Figure 5). The temperature, heat transfer coefficient, and incident flux profiles were assumed to be circular contours with values shown in Figure 6b, c, and d.

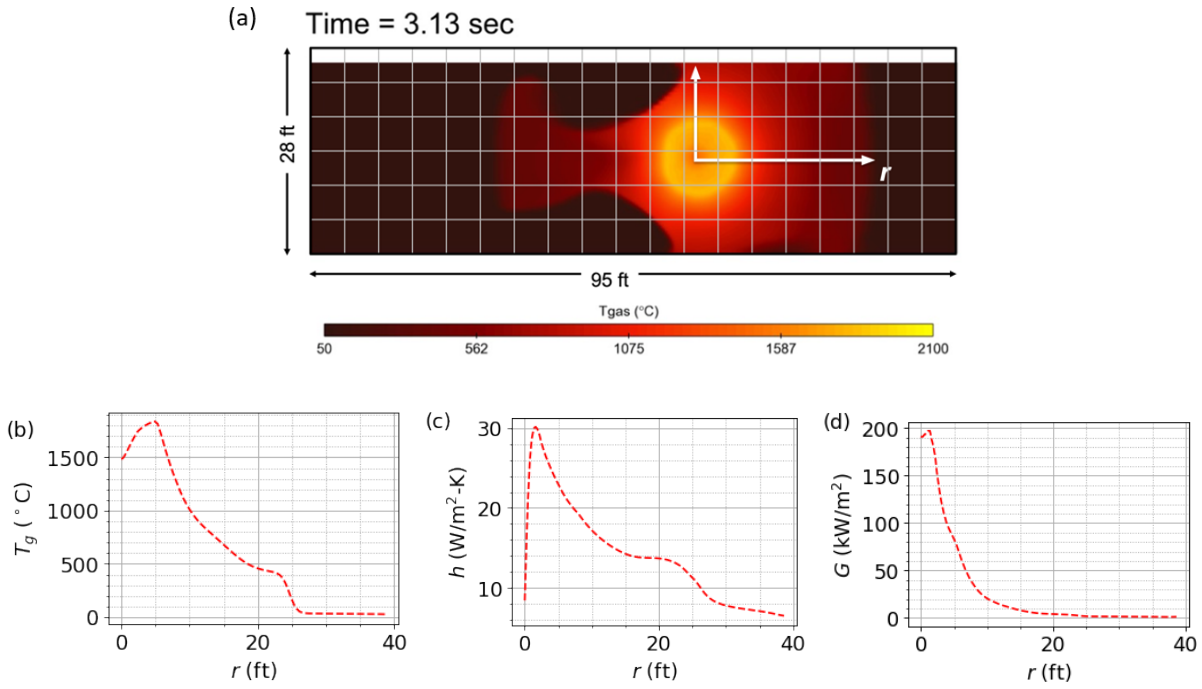

Figure 6. Boundary conditions applied on bottom surface of tunnel ceiling structure: (a) temperature map from [1], (b) the radial temperature, (c) convective heat transfer coefficient, and (d) irradiation plotted with respect to the r-axis measuring radial length from the center of the flame impingement at the bottom surface.

2.3. Mesh Refinement

A mesh refinement study was performed to ensure that the temperatures obtained across the slab are independent of the mesh size. A sufficiently fine mesh is required to accurately capture large temperature gradients. Since this heat transfer analysis primarily aims to observe how severely the heat penetrates the thickness of the slab, the thickness of the slab was finely discretized more than along its length or width. Thus, a mesh resolution study was performed until numerical results were independent of mesh resolution. Temperatures T_1-T_{21} were compared for different uniform interval sizes. The best interval size was selected once the temperatures T_1-T_{21} did not change when the interval size changes.

The number of intervals was refined from 12 to 30 intervals to select the interval size for the heat transfer simulations. Figure 7 shows the temperature as a function of time at the bottom surface (top-left), 1 in. (top-right), 1 ¾ in. (bottom-left), and 5 (bottom-right) from the bottom surface for intervals size of 12, 18, 22, 26, and 30. For interval greater than or equal to 26, the mesh was sufficiently fine for the results to be independent of the mesh size. The mesh selected for the heat transfer simulation consisted of 26 intervals along the thickness (as shown in Figure 8), resulting in 1,190,644 elements and 1,244,079 nodes.

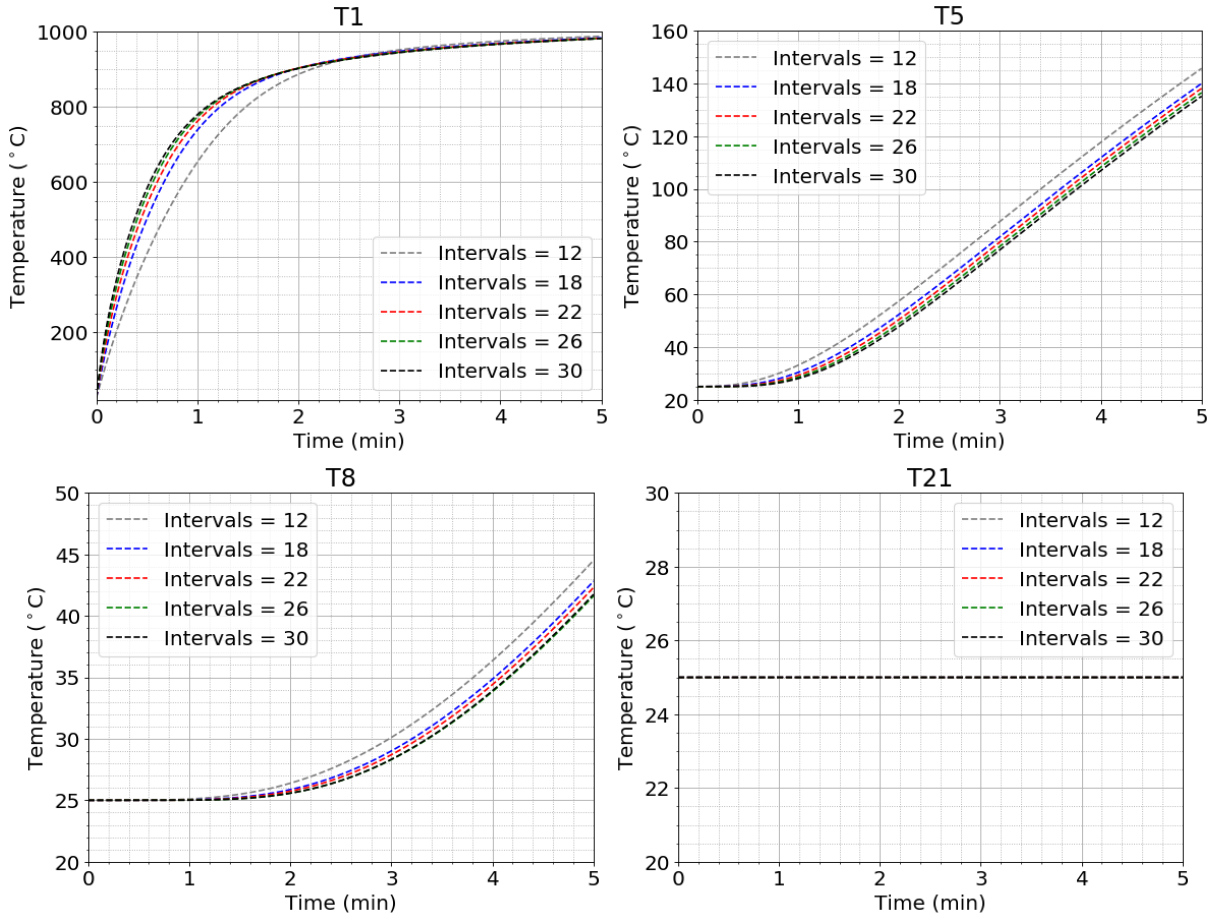

Figure 7. Temperature at y=0 (top-left), y=1 in. (top-right), 1.75 in. (bottom-left), and 5.5 in. (bottom-right) from the bottom surface for intervals 12 to 30. When the thickness is divided into 26 intervals or more, the mesh is sufficiently fine.

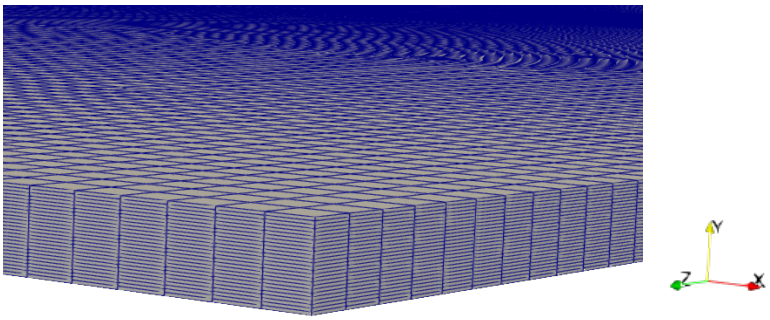

Figure 8. Isometric view of mesh for the lower concrete layer of the box beam using 26 intervals along the thickness of the concrete layer.

3. RESULTS

This section presents the results for the bottom concrete slab of the box beam. The temperature distributions on a vertical cross-sectional view perpendicular to the z-plane at z=0 are displayed for time t =0, 50 s, 1.3 minutes, and 5 minutes for each slab. The temperatures as a function of time at x =z = 0 for different y-locations are also presented. A vertical dash-dotted blue line is positioned at 50 seconds to indicate when the 5 kg of hydrogen have been fully released at the mass flow rate used in the CFD model. The other vertical dashed line at 1.3 minutes indicates when the flame is no longer impinging on the tunnel ceiling.

The temperature distribution at the z-plane cross-section, as well as the plots that show the transient temperature profiles at different locations along the thickness of the concrete slab are presented. The simulations accounted for changes in bulk density as temperature increased. However, the heat transfer simulations did not model mass loss due to spalling. Previous experimental work [6] was used to determine if explosive spalling is likely to happen. The authors in [6] found that explosive spalling can occur when concrete reaches temperatures higher than 750°C.

Figure 9 shows the temperature of the concrete slab when cut by a z-normal plane located at $z = 0$ for time t =0, 50 s, 1.3 min, and 5 min. The temperature at the bottom surface of the concrete slab increases rapidly. The maximum temperature increases from ambient temperature (25°C) to 750°C in 50 s. The maximum temperature reaches 848°C at 1.3 minutes. After 5 minutes, a more significant change can be observed along the thickness of the slab, and the maximum temperature reaches 1008°C. No temperature changes are observed at y = 5.5 in. Explosive spalling could happen very close to the bottom surface after 50 s of flame exposure, since temperature has reached 750°C.

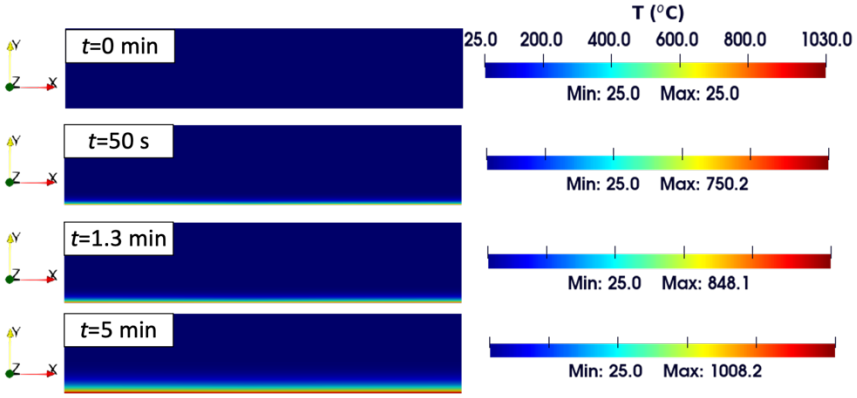

Figure 9. Temperature distribution across a 5.5 in. thick concrete slab at different time steps. From top to bottom: 0, 50 s, 1.3 min, and 5 min. Maximum and minimum values are specified for each time step.

Figure 10 shows the maximum temperature of the structure (red dashed line) for for the concrete slab in the box beam, which is always going to be at the bottom surface (y = 0). The rapid increase in maximum temperature of the slab can be observed in Figure 10a. A maximum temperature reaches 1008°C in 4 minutes and remains constant after that. The temperatures at x=z = 0 for different y-locations are also presented in Figure 10a and b. Figure 10b is a version of Figure 10a with a smaller y-axis temperature scale to show the increasing temperatures at locations y = 1.0 in. in purple and y = 1 ¾ in. in magenta from the bottom surface.

At 50 seconds, the maximum temperature increases from ambient temperature to 750°C. However, the temperature at 1 in. from the bottom surface is still at ambient temperature. At 1.3 minutes, the maximum temperature reaches 848°C, and the temperature at 1 in. from the surface has increased to 31 °C while the temperature at 1 ¾ in. remains at ambient. After 5 minutes, the bottom surface reaches a temperature of 1008°C. At only 0.25 in. (0.635 cm) from the bottom surface, a significantly lower temperature (560°C) can be observed after 5 minutes. At 0.5 in. (1.27 cm) from the bottom surface, the temperature has only reached a value of 350°C after 5 minutes. The temperature at 1 in. from the surface reaches 130°C while the temperature at 1 ¾ in. reaches 40°C (see Figure 10b).

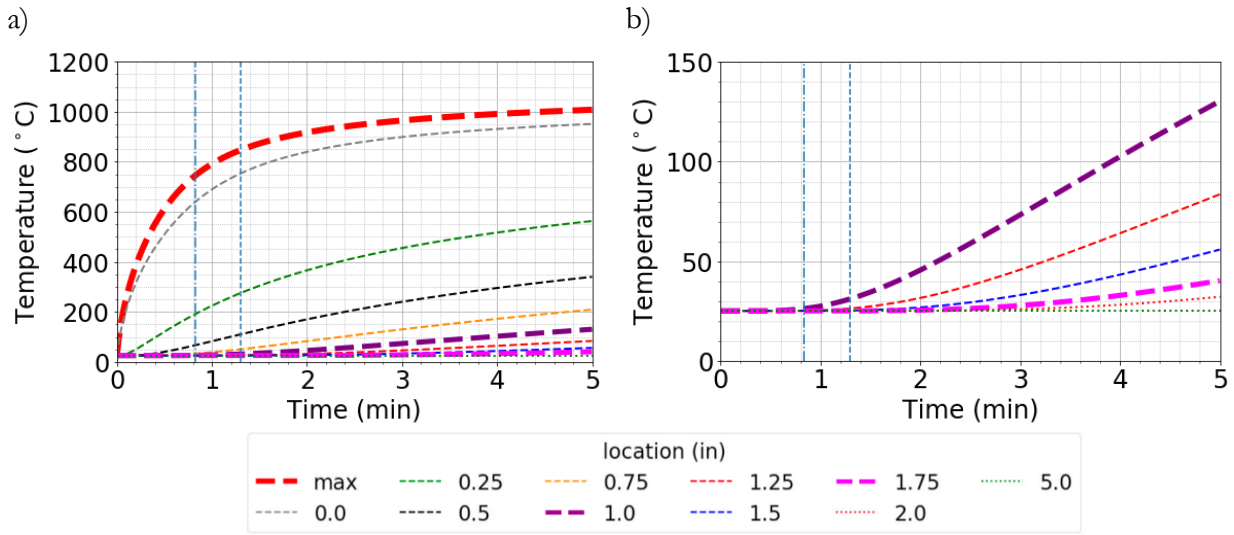

Figure 10. Transient temperature profiles for different y-locations at $x = z = 0$ for the concrete slab in box beam tunnel. The red-dashed line indicates the maximum temperatue of the concrete. Figure 10b is a version of Figure 10a with a smaller y-axis temperature scale to show the increasing temperatures at locations y= 1.0 in. in purple and y = 1 ¾ in. in magenta from the bottom surface to emphasize the location where the steel reinforcing bars are located.

Explosive spalling can occur where temperature reaches 750 °C. The analyses show that after 50 seconds, explosive spalling may affect a thin concrete layer of ~0.05 in. at the bottom of the concrete slab. However, the rest of the concrete slab should remain intact since temperatures remain below 750°C everywhere else throughout the slab. After 5 minutes, explosive spalling may still only affect the lower 0.1 in. layer of the concrete slab. Therefore, even if explosive spalling occurs, the steel reinforcing bars will be protected from the hydrogen flame by a ~0.9 in. thick layer of concrete. The removal of parts of the concrete from the spalling may increase the heat transfer through the rest of the concrete slab but not enough to reach the steel reinforcing bars. These times and depths of potential spalling are also affected by the conservatism in the model, as pointed out in Section 1.1 and 1.2.

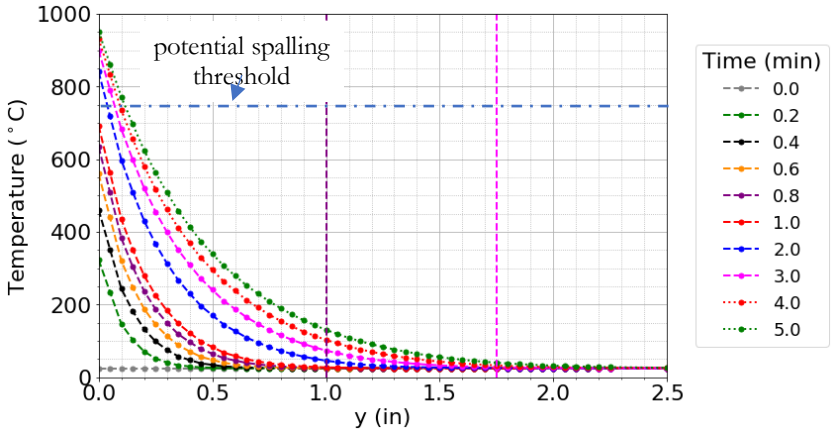

Figure 11. Temperature profiles across the thickness of the concrete slab in box beam at different time steps show that at y = 2 in. the temperature is still ambient. Locations y = 1.0 in. (purple) and y = 1 ¾ in. (magenta) are marked to show the location of the steel reinforcements.

4. SUMMARY AND CONCLUSIONS

This report examined a scenario where a FCEV is overturned when it crashes with a gasoline vehicle. The TPRD is activated when gasoline from a leak ignites, creating an engulfing fire. The hydrogen released encounters heat from the fire, causing the hydrogen jet to ignite. When modeling assumptions were needed, conservative values were used so that the assumptions overestimate instead of underestimating the heat transfer to the tunnel. These assumptions were mainly applied to the convective and radiative heat transfer boundary conditions at the lower surface of the box beam. The heat transfer coefficient, gas temperature, and incident heat flux obtained in the CFD simulations performed in [1] were used as boundary conditions in this study. The authors in [3] assumed a hydrogen release with constant mass flow rate for 5 minutes. This is a conservative assumption since the mass flow rate is expected to decrease with time resulting in a decrease in heat generation. In the CFD simulations, the amount of hydrogen that would be released in 5 minutes using a constant mass flow rate is 30 kg, not the 5 kg of a typical storage tank. The 5 kg of hydrogen would be released in the first 50 seconds of those simulations. Results for a duration of 5 minutes were presented, but temperatures at 50 seconds and 1.3 minutes should be noted.

This work investigated tunnel ceiling composed of steel reinforced concrete box beams. We assumed that the hydrogen jet flame impinges on the exposed bottom surface of the box beams. Only the lower layer of concrete was modeled to determine whether the heat reaches the steel reinforcing bars and whether concrete spalling can occur. There are two steel reinforcing bars along the length of the concrete box beams. The steel reinforcing bars are at 1 in. and 1 ¾ in. from the bottom surface of the bottom box beam.

Table 1 summarizes important temperature values at 50 seconds, 1.3 minutes, and 5 minutes for the lower concrete layer in the box beam simulation. The simulations showed that the steel reinforcing bars located at 1 in. from the bottom surface of the box beam remain approximately at ambient temperature for the first 1.3 minutes of the simulation. After 5 minutes, the temperature at 1 in. reaches 130°C. Even though this increase in temperature is not desirable, results for times after 50 seconds are overestimated since the 5 kg inside the tank are released within 50 seconds. The lower layer of concrete in the box beam slab is sufficient to maintain the steel reinforcing bars located at 1 ¾ in. at ambient temperature for 2.5 minutes. Even after 5 minutes, the temperature at 1 ¾ in. only reaches 40°C.

Explosive spalling was not included in our model. However, we used Ali et al. [6] observations on their concrete explosive spalling experiments to determine whether explosive spalling is likely to happen for the temperatures listed in Table 1. Ali et al. [6] observed explosive spalling when the concrete reached 750°C. Even though the concrete used by Ali et al. [6] may not have the same properties from the box beam, the properties will be similar enough to assess whether spalling should be a concern.

After 50 seconds, only a thin layer (~0.05 in.) reaches a maximum temperature of 750°C, so explosive spalling may occur at that thin layer, which is localized where the flame impinges on the concrete box beam. However, the rest of the concrete slab should remain intact since temperatures remain below 750°C everywhere else. After 5 minutes, explosive spalling maybe observed at a 0.1 in. layer at the bottom surface of the concrete slab. Even if explosive spalling occurs, the steel reinforcing bars will still be protected from the hydrogen flame by a ~0.9 in. thick layer of concrete. As noted, results for potential spalling past the 50 second mark in the release time should be used with caution as they are overestimated and conservative due to the modeled release of more than 5 kg of hydrogen.

Even though the concrete surface exceeded 380°C and was not completely protected from fire-induced spalling as recommended by NFPA 502 for gasoline, one should keep in mind that the fire is for a very short time (compared to gasoline fires), so only a very thin layer of concrete will reach the spalling temperature. In addition, gasoline fires will heat up a larger area than the area the hydrogen flame will heat up. NFPA 502 also recommended the temperature of the steel reinforcements within the concrete to not exceed 250°C. The results in this work showed that the steel reinforcements stayed near ambient temperature.

The authorities having jurisdictions in tunnels with a similar box beam ceiling can use the findings of this work to determine whether the integrity of their tunnel will be compromised under the extremely low probability of an impinging hydrogen jet flame from a TPRD release. The concrete, the box beam dimensions, or the location of the steel reinforcing bars in their tunnel may differ from the one selected for this work. However, if the concrete thermal properties are similar, a similar thermal behavior can be expected. If the geometry of the box beam or location of steel reinforcing bars are different, this work can still be used to find the temperature at different locations in the lower layer of the box beam. ACI/TMS 216.1-14 provides temperature dependent strength curves for several types of concrete and steel reinforcing bars, which can be used to determine whether the steel reinforcing bars will permanently deform or fracture. To ensure that the findings of this report can be used to assess a specific tunnel, the assumptions and tunnel conditions used in this work should be carefully reviewed.

Table 1. Summary of temperatures of the box beam tunnel at t = 50 seconds, 1.3 minutes, and 5 minutes.

Time	Temperature (^{O}C)					
	Min. ***(y* = 5.5 in.)**	**Max.** ***(y* = 0)**	**Center at Bottom Surface** ***(x* = *y* = *z* = 0)**	**Center at *y* = 1 in.** ***(x* = *z* = 0)**	**Center at *y* = 1.75 in.** ***(x* = *z* = 0)**	**Top Surface at *y* = 5.5 in.** ***(x* = *z* = 0)**
50 s	25.0	747.6	642.2	26.2	25.0	25.0
1.3 min	25.0	846.8	753.1	31.0	25.0	25.0
5.0 min	25.0	1008.2	951.5	130.3	40.2	25.0

REFERENCES

1. *U.S. National Clean Hydrogen Strategy and Roadmap*. 2023, U.S. Department of Energy.
2. *NFPA 502: Standard for Road Tunnels, Bridges, and Other Limited Access Highways*. 2023, National Fire Protection Association (NFPA).
3. LaFleur, C.B., et al., *Hydrogen Fuel Cell Electric Vehicle Tunnel Safety Study*. 2017, Sandia National Laboratories Report SAND2017-11157.
4. *SIERRA Multimechanics Module: Aria User Manual (V.5.0)*. 2021: Sandia National Laboratories Report SAND2021-3921.
5. *ACI CODE-216.1-14(19). Code Requirements for Determining Fire Resistance of Concrete and Masonry Construction Assemblies*. 2014, Joint ACI/TMS Comm 216: American Concrete Institute.
6. Ali, F., A. Nadjai, and A. Abu-Tair, Explosive spalling of normal strength concrete slabs subjected to severe fire. Materials and structures, 2011. 44: p. 943-956.
7. *Typical Deck Section and Box Beam Details*. 1980, Parson Brinckerhoff: Boston, Massachusetts.
8. Standardisation, E.C.f., *Eurocode 3: Design of Steel Structures-Part 1-2: General Rules-Structural Fire Design*. 2007: London.

DISTRIBUTION

Email—Internal

Name	Org.	Sandia Email Address
Kristin Hertz	8367	klhertz@sandia.gov
Myra Blaylock	8751	mlblayl@sandia.gov
Gabriela Bran Anleu	8751	gabrana@sandia.gov
Camron Proctor	8751	cproct@sandia.gov
Brian Ehrhart	8854	bdehrha@sandia.gov
Chris LaFleur	8854	aclafle@sandia.gov
Marina Miletic	8854	mmileti@sandia.gov
Benjamin Schroeder	8854	bbschro@sandia.gov
Technical Library	1911	sanddocs@sandia.gov

Email—External

Name	Company Email Address	Company Name
Christina Felipe	chtfelipe@gmail.com	FM Global
Haider Hamandi	haider.hamandi@dot.state.ma.us	Massachusetts Department of Transportation
Laura Hill	laura.hill@ee.doe.gov	DOE HFTO
Charles Myers	cmyers@massh2.org	Massachusetts Hydrogen Coalition, Inc.
Andrew Paul	andrew.paul@dot.state.ma.us	Massachusetts Department of Transportation
Joseph Rigney	rigney@delveunderground.com	Delve Underground

This page left blank

Sandia National Laboratories

Sandia National Laboratories is a multimission laboratory managed and operated by National Technology & Engineering Solutions of Sandia LLC, a wholly owned subsidiary of Honeywell International Inc. for the U.S. Department of Energy's National Nuclear Security Administration under contract DE-NA0003525.